Competition between proton transfer and hydride abstraction in chemical ionisation mass spectrometry of ethylamine

Elisabeth Leere Øiestad, Einar Uggerud*

Department of Chemistry, University of Oslo, P.O. Box 1033 Blindern, N-0315 Oslo, Norway

Abstract

The reactions between ethylamine and two different proton donors (protonated water and protonated molecular nitrogen) have been investigated experimentally and theoretically. Proton transfer to the amino group yields protonated ethylamine, which may subsequently fragment via four different unimolecular reaction channels (loss of NH_3, C_2H_4, CH_4, and H_2). However, the observed losses of CH_4 and H_2 are better explained by mechanisms where CH_3^- and H^-, respectively, are abstracted directly in an encounter between the proton donor and ethylamine. (Int J Mass Spectrom 199 (2000) 91–105) © 2000 Elsevier Science B.V.

Keywords: Proton transfer; Hydride abstraction; *Ab initio* quantum chemistry; Fourier transform ion cyclotron resonance (FTICR), Ethylamine; Deuterium labeling

1. Introduction

The technique of chemical ionisation (CI) was established in 1966 by Munson and Field [1]. Since then many gas phase studies of the processes leading to a CI mass spectrum have been undertaken [2]. The key step in CI mass spectrometry (and also in electrospray ionisation and a number of modern plasma ionisation techniques) is the formation of the protonated form of the molecule, M:

$$AH^+ + M \rightarrow A + MH^+ \qquad (1)$$
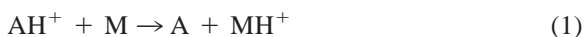
The protonated molecule may subsequently fragment via unimolecular reaction paths:

$$MH^+ \rightarrow F_1^+ + N_1 \rightarrow F_2^+ + N_2, \text{ etc.} \qquad (2)$$
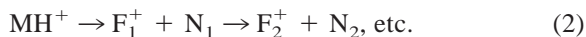
A molecule may have more than one basic site, thereby giving rise to isomeric forms of MH^+, each with a characteristic set of unimolecular reactions.

During an investigation of the CI of a series of protonated amines we became gradually aware of an alternative outcome to the encounter between a proton donor and a basic molecule. It turns out that hydrogen atoms and even complete alkyl groups are susceptible to proton attack. It seems as if formation of the corresponding MH^+ isomer is only transient in these cases because attack on a hydrogen leads to immediate dihydrogen formation

$$AH^+ + M \rightarrow (M - H)^+ + H_2 + A \qquad (3)$$
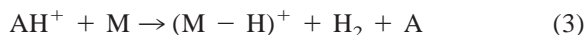
* Corresponding author. E-mail: einar.uggerud@kjemi.uio.no
Dedicated to Professor Henri Edouard Audier on the occasion of his 60th birthday.

and attack on a carbon leads to alkane formation. Hydride and alkyl anion abstraction reactions are described previously in the literature [2–11]—especially in connection with the CI of alkanes—but the present work represents to our knowledge the first detailed mechanistic study of these processes. Good examples and a more general literature review is given by Mathias *et al*. in their article (this issue) [12].

We decided to use ethylamine as our model system for the following reasons: (1) Protonated ethylamine may give rise to as many as four different unimolecular fragmentations. This provides a sensitive measure of the energetics. (2) Protonated ethylamine is a relatively small molecule, which facilitates high level *ab initio* calculations, that may help in clarifying the experimental findings. (3) The unimolecular reactions of protonated ethylamine have been studied in great detail previously [13].

Here we report the results of investigations of the potential energy surfaces of the molecular supersystems H_3O^+/$CH_3CH_2NH_2$, N_2H^+/$CH_3CH_2NH_2$, and $CH_3CH_2NH_3^+$. Both theoretical (quantum chemistry models) and experimental (Fourier transform ion cyclotron resonance mass spectrometry) methods were used.

2. Experimental

The experiments were carried out using a Fourier transform ion cyclotron resonance (FTICR) mass spectrometer with an external electron impact/chemical ionisation (EI/CI) ion source (Apex 47e, Bruker Daltonics, Billerica, MA). H_3O^+ (D_3O^+) and N_2H^+ (N_2D^+) were generated in the external ion source under CI conditions with a source pressure of 10^{-5} mbar. The source temperature was 384 K and the filament current was 3.8 A. In the case of water (HPLC grade, Rathburn, UK) and deuterium oxide (99.9% D, Fluorochem Ltd., UK) methane (99.995%, AGA, Norway) or d4 methane (99% D, CDN isotopes, Canada) were used as the CI reagent gas, whereas N_2 (99.99%, AGA, Norway) was reacted directly with H_2 (99.9997%, AGA, Norway) or D_2 (>99.8%, Hydrogas, Norway).

The CI products were transferred to the ICR cell, and the proton/deuteron donor was isolated by correlated frequency sweep [14]. The trapping plate voltages were held at 1 V, and all transfer parameters had small offsets only. The temperature of the cell was estimated to be approximately 300 K. Ethylamine (>99%, Fluka, Switzerland) was leaked into the ICR cell via a leak valve and held at a constant pressure of 2.5×10^{-9} mbar, as measured directly on the pressure gauge. The corresponding partial pressure of ethylamine was estimated to be ~0.8×10^{-9} mbar. The low pressure was chosen to avoid reaction during isolation. Using collisional rates obtained by the parametrized model of Su and Chesnavich [15], the collision frequency can be estimated to be 0.05 s^{-1} and 0.04 s^{-1} for H_3O^+ and N_2H^+, respectively. Spectra were recorded after a reaction time of 20 s that, therefore, represents approximately single collision conditions. One should realise that this allows 30% of the ions (protonated ethylamine and fragments) to collide with ethylamine. This fact and the leakage of isotope substituted reagents into the cell were accounted for in the data analysis.

The labeled ethylamine derivatives, $CH_3CD_2NH_2$, $CD_3CH_2NH_2$, and $CD_3CD_2NH_2$ were prepared by reduction of CH_3CN by $LiAlD_4$ (>99% D, Fluka, Switzerland), CD_3CN (>99.8% D, Cambridge Isotope Laboratories, MA) by $LiAlH_4$ and CD_3CN by $LiAlD_4$, respectively.

2.1. Synthesis of deuterated ethylammonium chloride

A slurry of 0.15 moles $LiAlH_4$($LiAlD_4$) in 100 ml dry ether was heated to reflux under a nitrogen atmosphere. A solution of 0.1 moles CD_3CN(CH_3CN) in 20 ml dry ether was then added dropwise to maintain a weak reflux without heating, followed by reflux for 1 h. After cooling, 30 ml of water were added dropwise while stirring vigorously. The gas formed was bubbled through 200 ml 1 M HCl and the water/HCl was then evaporated to give ethylammonium chloride as a white crystalline product. The obtained yield was 60–70%.

2.2. Preparation of deuterated ethylamine

A solution of 5 g NaOH in 5 ml water was added per 0.1 mol grounded ethylammonium chloride while stirring the solution. The ethylamine formed was condensed at −78 °C. Heating of the mixture in a water bath at 40 °C for 3 h gave a yield of 70–80% ethylamine. The isotopic purity of the compounds was determined by ^{1}H NMR and/or CI mass spectrometry to be >95%.

3. Theoretical methods

Quantum chemical calculations were carried out using the program system GAUSSIAN 94 [16]. The methods used were Møller–Plesset [17] perturbation theory to the second (MP2) order with a 6-31G(d,p) basis set and the composite G2 method [18].

All stationary points found on the potential energy surface were characterised by complete optimisation of the molecular geometry for MP2. Harmonic frequencies were obtained from the diagonalized mass-weighed Cartesian force constant matrix, calculated from the analytical second derivatives of the total energy (the Hessian). The zero point vibrational energies (ZPVE) calculated from the MP2/6-31G(d,p) harmonic frequencies were scaled by a factor [19] of 0.9608 and included in the total energies. For the total energies calculated by the G2 method [18] the built-in scale factor was used for the ZPVE. The results are presented in Table 1 and geometrical parameters from the MP2/6-31G(d,p) calculations are depicted in Fig. 1. Intrinsic reaction coordinate calculations were used to connect the transition structures with the correct reactants and products.

4. Results and discussion

4.1. General

As already mentioned in the introduction there are two different routes to fragment formation in proton transfer reaction: (1) Proton transfer to M giving MH^+. Subsequently, and separated in time and space, the MH^+ ion decomposes unimolecularily. (2) Proton transfer to M, whereupon fragmentation takes place immediately.

For route (1) it is important to consider the energetics of the two steps. The fragmentation is steered by the amount of energy deposited into MH^+ upon formation. The proton affinity, PA(M), is an important parameter in this context. It is a measure of the basicity and is defined as the negative enthalpy change for the reaction

$$M + H^+ \rightarrow MH^+, \quad PA(M) = -\Delta H^0 \tag{4}$$

In a proton transfer reaction the maximum amount of internal energy that can be transferred to MH^+, E_{max}, is equal to the difference in proton affinity between the proton donor and acceptor:

$$E_{max} = PA(M) - PA(A) \tag{5}$$

Two different proton donors (protonated water and protonated dinitrogen) were selected—a weak and strong proton donor, respectively. Ethylamine itself is a strong proton acceptor. The proton affinities [20] are $PA(H_2O) = 691$ kJ mol^{-1}, $PA(N_2) = 494$ kJ mol^{-1}, and $PA(C_2H_7N) = 912$ kJ mol^{-1} giving $E_{max} = 221$ kJ mol^{-1} and $E_{max} = 418$ kJ mol^{-1} for H_3O^+ and N_2H^+, respectively. The observed reactions indicate the extent to which the available energy ends up as internal energy in MH^+. The internal energy of MH^+ is available for further fragmentation, whereas energy that ends up in translational or rotational modes or as internal energy in A is inaccessible for reaction.

4.2. Theoretical model

4.2.1. Direct bimolecular reactions

Depending on energy and relative orientation, an encounter between ethylamine and a proton donor, AH^+, may give either proton transfer, methide (methyl anion) abstraction, or hydride abstraction:
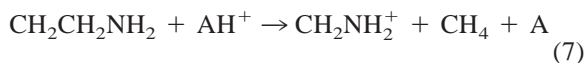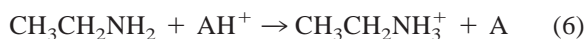
$$CH_3CH_2NH_2 + AH^+ \rightarrow CH_3CH_2NH_3^+ + A \tag{6}$$

$$CH_2CH_2NH_2 + AH^+ \rightarrow CH_2NH_2^+ + CH_4 + A \tag{7}$$

Table 1
Total energies from *ab initio* calculations including zero point energies

Structure	MP2/6-31G(d,p)[a] (Hartrees)	G2 (0 K)[b] (Hartrees)
1 $CH_3CH_2NH_2$	−134.64315	−134.89458
2 H_3O^+	−76.47221	−76.59193
3 $CH_3CH_2NH_3^+ \cdots H_2O$	−211.22954	−211.59792
4 $CH_3CH_2NH_3^+$	−134.99928	−135.24044
5 H_2O	−76.19877	−76.33205
6 $CH_2NH_2^+$	−94.63810	−94.79185
7 CH_4	−40.31990	−40.41091
8 H_2	−1.14757	−1.16636
9 $CH_3CHNH_2^+$	−133.81559	−134.04107
10 $\overline{CH_2CH_2NH_2^+}$	−133.78536	−134.00794
11 N_2H^+	−109.43317	−109.57856
12 $CH_3CH_2NH_3^+ \cdots N_2$	−244.25755	−244.64022
13 N_2	−109.25052	−109.39263
14 $NH_4^+ \cdots CH_2CH_2$	−134.96940	−135.21325
15 CH_2CH_2	−78.26699	−78.41593
16 NH_4^+	−56.68478	−56.78140
17 $CH_2NH_2^+ \cdots CH_4$	−134.96254	−135.20850
18 $C_2H_5^+ \cdots NH_3$	−134.90619	−135.15332
19 $C_2H_5^+$	−78.53066	−78.67412
20 NH_3	−56.34915	−56.45865
21 $CH_3CHNH_2^+ \cdots H_2$	−134.96304	−135.20817
22 $\overline{CH_2CH_2NH_2^+} \cdots H_2$	−134.93278	−135.17434
23 $\overline{CH_2CH_2NH_2^+} \cdots H_2$	−134.93316	−135.17623
24 $CH_2CHNH_3^+ \cdots H_2$	−134.93879	−135.18573
25 $CH_2CHNH_3^+$	−133.79113	−134.01761
TS(3/5+6+7)	−211.10911	−211.48353
TS′(3/5+6+7)	−211.10869	−211.48258
TS″(3/5+6+7)	−211.10792	−211.48108
TS(3/5+8+9)	−211.12842	−211.50523
TS(3/5+8+10)	−211.08613	−211.46450
TS(12/6+7+13)	−244.13021	−244.52087
TS′(12/6+7+13)	−244.12548	−244.51725
TS(12/8+9+13)	−244.13092	−244.52502
TS(12/8+10+13)	−244.11629	−244.51010
TS(4/14)	−134.87645	−135.15499
TS(4/17)	−134.90805	−135.12328
TS(4/21)	−134.86834	−135.11671
TS(4/22)	−134.85964	−135.11156
TS(4/23)	−134.84002	−135.09410
TS(4/24)	−134.80088	−135.05321

[a] Zero point energy scaled by 0.9608.
[b] Zero point energy scaled by the built-in scale factor.

$$CH_3CH_2NH_2 + AH^+ \rightarrow C_2H_6N^+ + H_2 + A \quad (8)$$
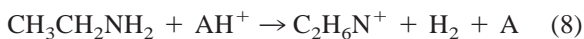
The ion $C_2H_6N^+$ can be formed by removal of a hydrogen from either the α or β carbon, giving protonated acetaldimine (**9**) or protonated aziridine (**10**), respectively.

The calculated G2 potential energy diagram with H_3O^+ as proton donor is depicted in Fig. 2. According to calculations the proton transfer, reaction (6), is exothermic by 226 kJ mol^{-1}. This is in good agreement with the experimental figure of 221 kJ mol^{-1}. It takes place via the hydrogen bonded complex (**3**),
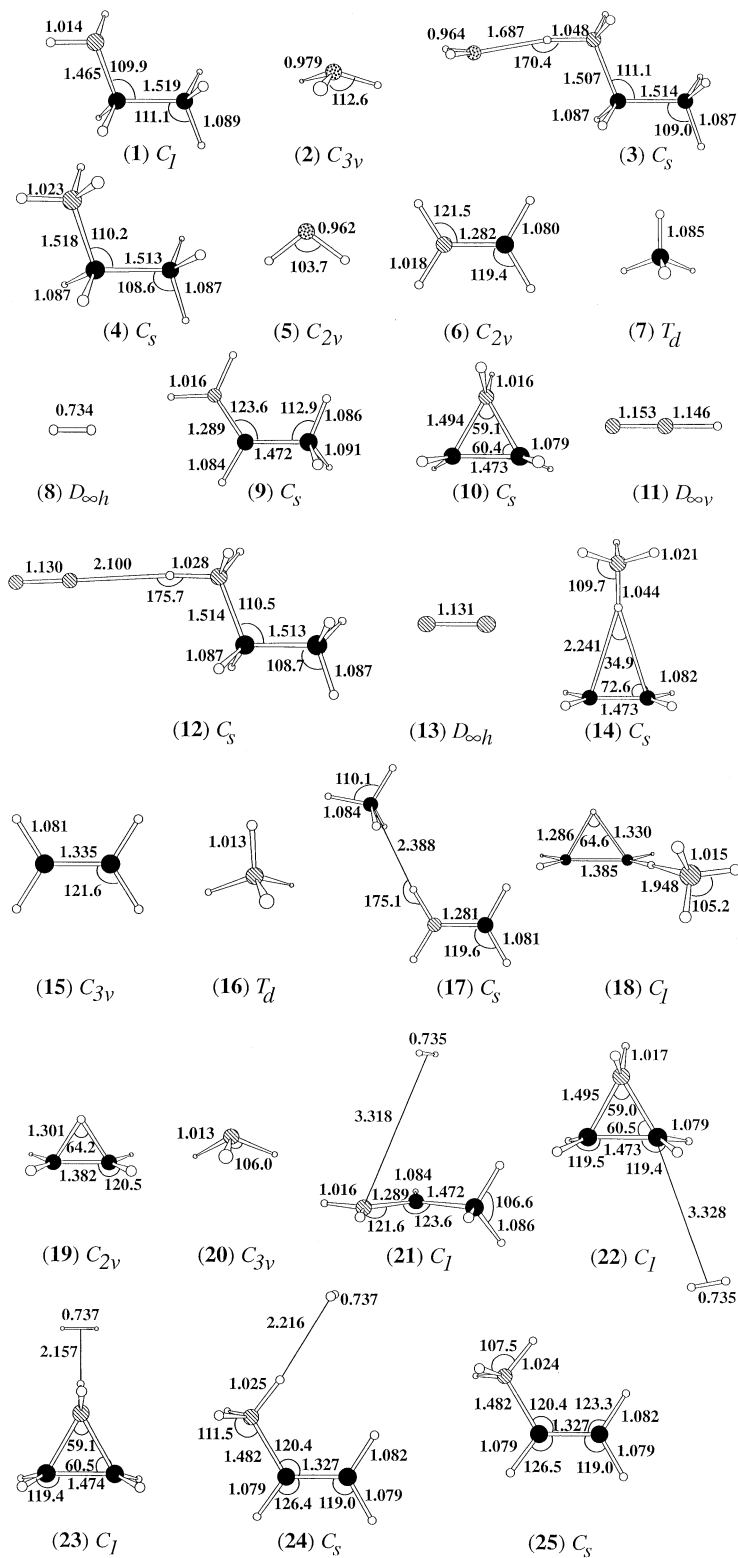
Fig. 1. Geometrical structures of reactants, transition structures, and intermediates of the $H_3O^+/CH_3CH_2NH_2$, $N_2H^+/CH_3CH_2NH_2$, and $CH_3CH_2NH_3^+$ systems computed with MP2/6-31G(d,p). The carbon atom is marked with black, the nitrogen atom by stripes, the oxygen atom by spots, and the hydrogen atom by an open circle. Bond distances are given in angstroms and angles in degrees.
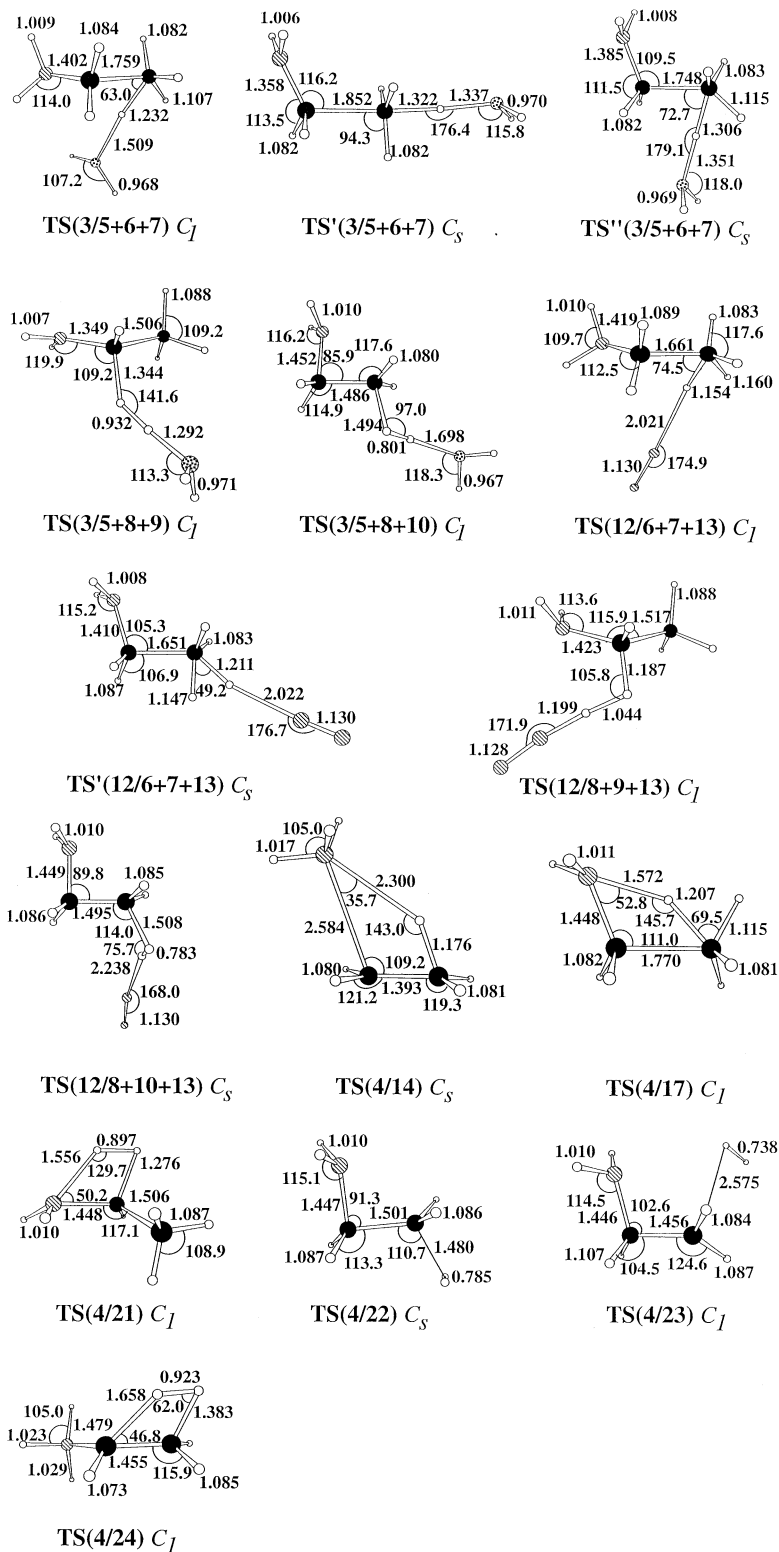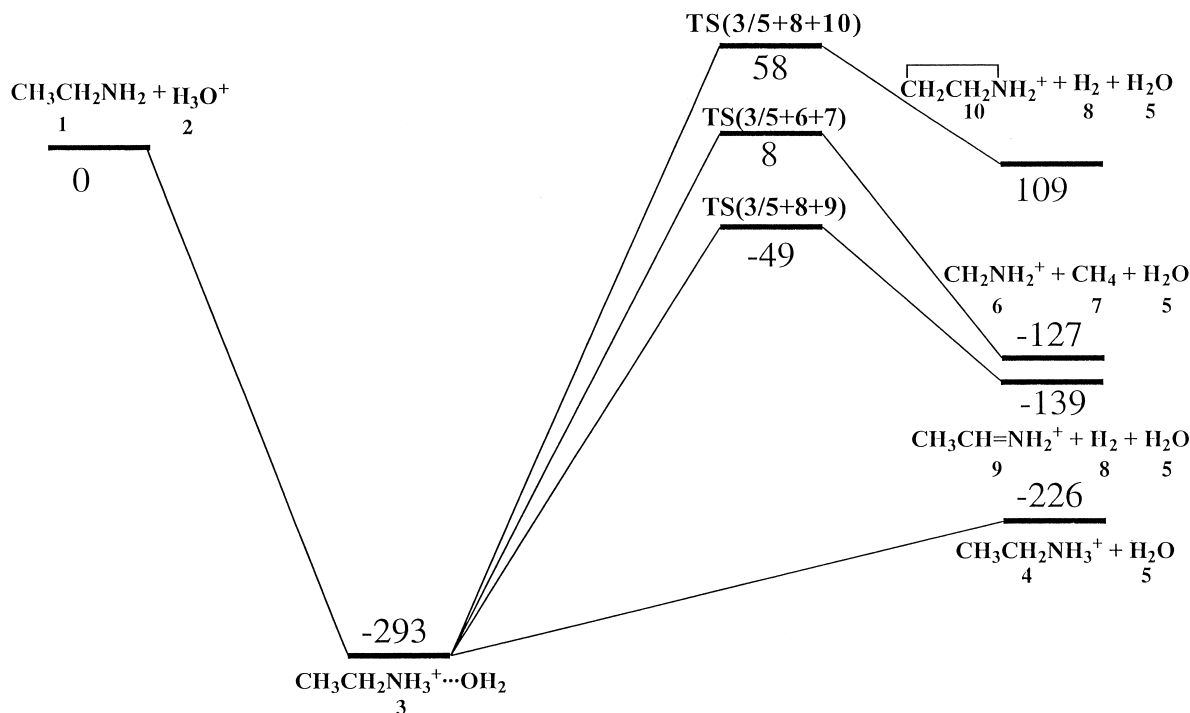
TS(3/5+6+7) C_1 TS'(3/5+6+7) C_S TS''(3/5+6+7) C_S

TS(3/5+8+9) C_1 TS(3/5+8+10) C_1 TS(12/6+7+13) C_1

TS'(12/6+7+13) C_S TS(12/8+9+13) C_1

TS(12/8+10+13) C_S TS(4/14) C_S TS(4/17) C_1

TS(4/21) C_1 TS(4/22) C_S TS(4/23) C_1

TS(4/24) C_1

Fig. 1. (continued)

Fig. 2. G2 potential energy diagram depicting the $H_3O^+/CH_3CH_2NH_2$ system. Relative energies indicated are in kJ mol^{-1}.
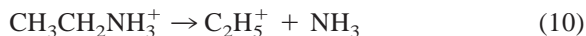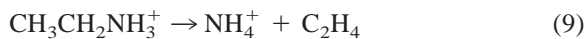
which represents the potential energy minimum. The transition structure for abstraction of the α hydrogen (in the form of a hydride), structure **TS(3/5 + 8 + 9)**, is 49 kJ mol^{-1} below the reactants, whereas the transition structure for abstraction of the β hydrogen, structure **TS(3/5 + 8 + 10)**, is 58 kJ mol^{-1} above. Three different transition structures for the methide abstraction, reaction (7), were found: **TS(3/5 + 6 + 7)**, **TS′(3/5 + 6 + 7)**, and **TS″(3/5 + 6 + 7)**. They are all within a few kJ mol^{-1} of each other in energy and only the lower energy, **TS(3/5 + 6 + 7)**, is shown in Fig. 2. The transition from the reactants to **TS(3/5 + 6 + 7)** proceeds with a barrier of only 8 kJ mol^{-1}.

Fig. 3 shows the calculated potential energy diagram (G2 values) when the proton donor is N_2H^+. Proton transfer [reaction (6)] is exothermic by 418 kJ mol^{-1}(exp.)/420 kJ mol^{-1}(G2). The proton bonded complex (**12**) between nitrogen and protonated ethylamine is only 19 kJ mol^{-1} more stable than free nitrogen (**13**) and protonated ethylamine (**4**). Two

transition structures were found for the methide abstraction, **TS(12/6 + 7 + 13)** and **TS′(12/6 + 7 + 13)**, differing in energy by 12 kJ mol^{-1}. The transition structures **TS(12/8 + 9 + 13)** and **TS(12/8 + 10 + 13)** were found for hydride abstraction. Both methide and hydride abstraction are exothermic, and the calculated barriers indicate that both methide and α- and β-hydrogen abstraction are energetically feasible.

4.2.2. Unimolecular reactions subsequent to protonation
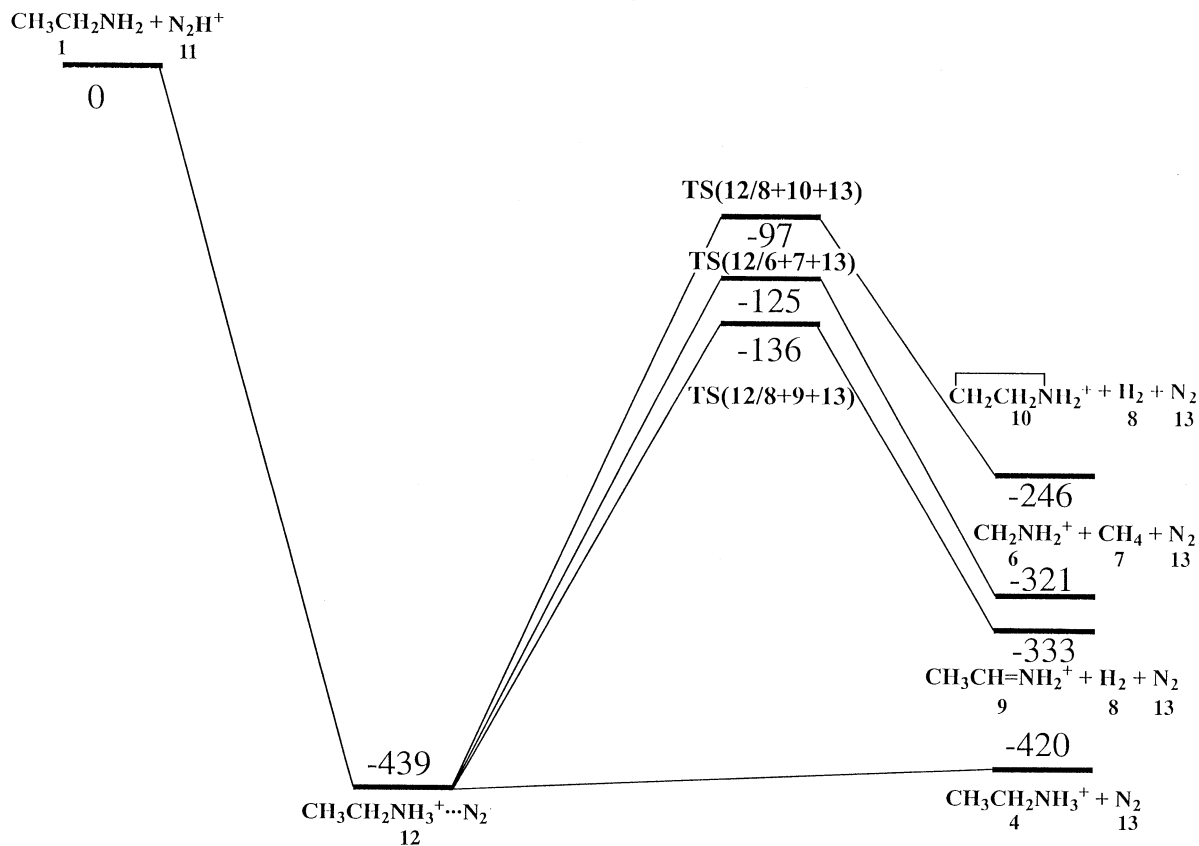
Protonated ethylamine may fragment by reactions (9)–(12):

$$CH_3CH_2NH_3^+ \rightarrow NH_4^+ + C_2H_4 \tag{9}$$

$$CH_3CH_2NH_3^+ \rightarrow C_2H_5^+ + NH_3 \tag{10}$$

$$CH_3CH_2NH_3^+ \rightarrow CH_2NH_2^+ + CH_4 \tag{11}$$

$$CH_3CH_2NH_3^+ \rightarrow C_2H_6N^+ + H_2 \tag{12}$$
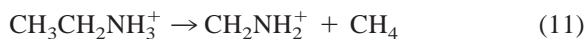
Fig. 3. G2 potential energy diagram depicting the $N_2H^+/CH_3CH_2NH_2$ system. Relative energies indicated are in kJ mol^{-1}.

Analogous reaction channels have been found for the unimolecular dissociation of the isoelectronic ion protonated ethanol [21,22]. From our theoretical calculations (Fig. 4), the lowest energy fragmentation process is reaction (9), formation of NH_4^+ (**16**) via **TS(4/14)** at 224 kJ mol^{-1}. The direct cleavage to $C_2H_5^+$ (**19**) and NH_3 (**20**), reaction (10), is at 283 kJ mol^{-1}, whereas reaction (11), loss of methane (**7**) to yield $CH_2NH_2^+$ (**6**), proceeds via **TS(4/17)** at 308 kJ mol^{-1}. The results for reaction (9) and (10) compare nicely to those calculated by Bouchoux *et al*. [13], whereas reactions (11) and (12) were not explicitly considered in their study.

Earlier studies of protonated ethylamine [13] and the isoelectronic system of protonated ethanol [21,22] have shown that there may exist other mechanisms for reaction (10) in addition to the obvious direct bond scission. A complex $[C_2H_5^+ \cdots NH_3]$ (**18**) lower in energy than the separated products $C_2H_5^+$ and NH_3 may participate in the loss of ammonia as discussed by Bouchoux *et al*. [13].

In the isoelectronic system of protonated ethanol [21,22], both losses of water and ethene are found to follow decomposition pathways via the same transition structure and complex that in our study would correspond to **TS(4/14)** and $[CH_2CH_2 \cdots H \cdots NH_3]^+$ (**14**). A possible decomposition route through the low energy complex (**14**) should therefore also be considered. The amount of hydrogen scrambling would be indicative of the participation of an intermediate complex, and we will return to this point in the discussion of the experimental results.
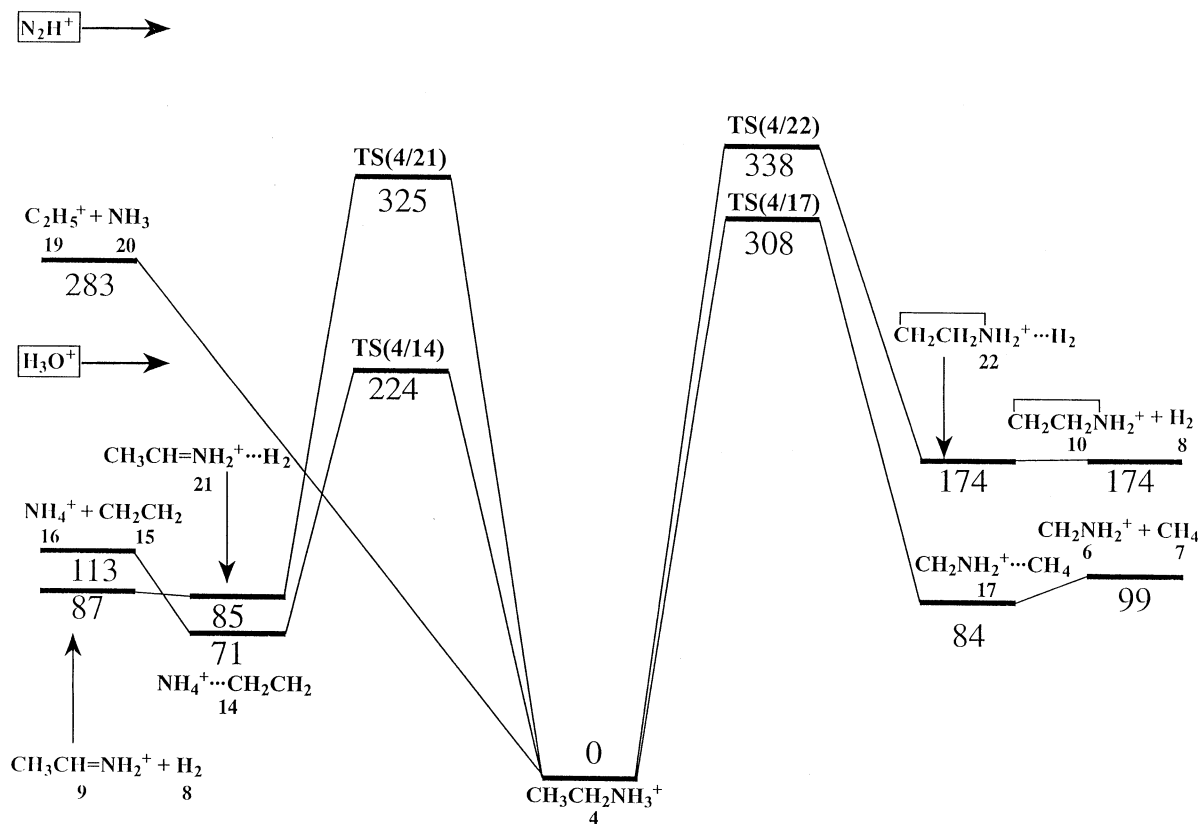
For the unimolecular H_2 elimination from proto-

Fig. 4. G2 potential energy diagram showing unimolecular pathways from protonated ethylamine. The arrows indicate the exothermicity for protonation by the proton donors H_3O^+ and N_2H^+. Relative energies indicated are in kJ mol^{-1}.

nated ethylamine [reaction (12)], three possible pathways exist: 1,2 elimination yielding protonated acetaldimine (**9**), 1,3 elimination yielding protonated aziridine (**10**), and 2,3 elimination yielding protonated vinylamine (**25**). The H_2 elimination pathway that is lowest in energy is the 1,2 elimination. It proceeds via **TS(4/21)** at 325 kJ mol^{-1}. The transition structure closely resembles the 1,2 H_2 elimination from protonated ethanol calculated by Swanton *et al.* [21]. Two different transition structures were found for the 1,3 elimination, **TS(4/22)** and **TS(4/23)**. Both **TS(4/23)** and the transition structure for 2,3 elimination, **TS(4/24)**, have very high energy barriers and are therefore left out of Fig. 4. Weakly bonded complexes between molecular hydrogen and the different structures of $C_2H_6N^+$, **21–24**, were found for all four transition structures leading to H_2 elimination.

4.3. Experimental results

The mass spectrum obtained in the reaction between H_3O^+ and ethylamine is shown in Fig. 5, and that of the reaction between N_2H^+ and ethylamine in Fig. 6. As expected, more fragmentation takes place when more energy is available (N_2H^+). Both spectra show that losses of C_2H_4, NH_3, H_2, and CH_4 take place. In the case where N_2H^+ is the proton donor all four fragments could, in principle, be the result of the proton transfer/unimolecular decomposition route. With H_3O^+ as the proton donor, however, the high energy processes for H_2 and CH_4 loss should not be energetically accessible unimolecularily (Fig. 4). The observation of H_2 and CH_4 losses in the reaction between H_3O^+ and $CH_3CH_2NH_3^+$ is therefore a clear indication of direct bimolecular reactions.
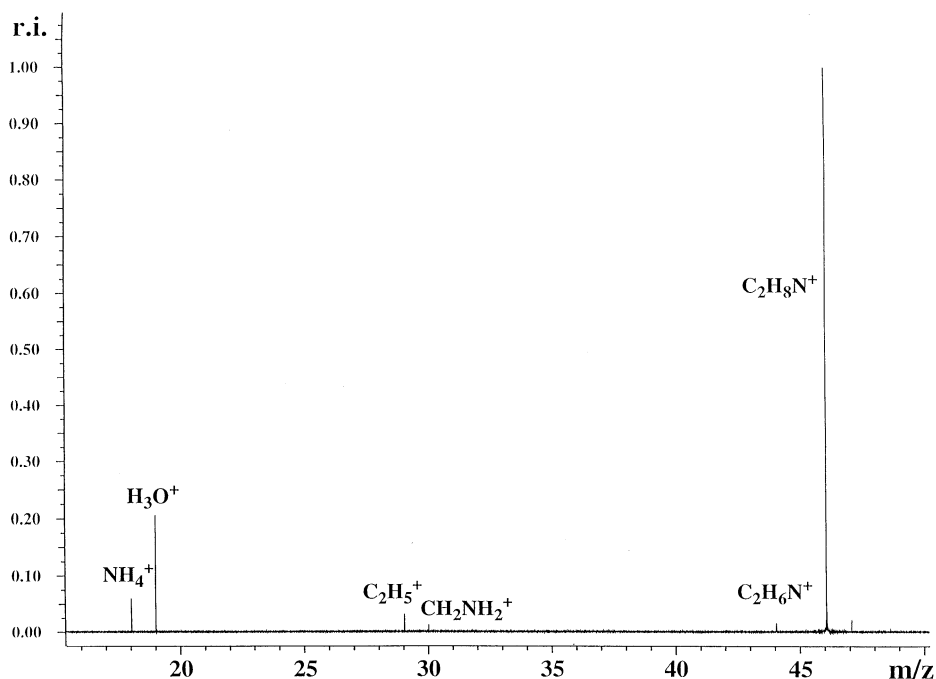
Fig. 5. Mass spectrum obtained after 20 s in the reaction between H_3O^+ and ethylamine.

To look more directly into the mechanistic landscape, deuterium labeling was performed. A total of 16 reactions between the proton donors H_3O^+, D_3O^+, N_2H^+, and N_2D^+ and the ethylamines $CH_3CH_2NH_2$, $CH_3CD_2NH_2$, $CD_3CH_2NH_2$, and $CD_3CD_2NH_2$ were investigated to obtain as complete a picture as possible of the mechanisms involved.

4.3.1. The NH_4^+ and $C_2H_5^+$ ions

The NH_4^+ ion results from the lowest energy fragmentation pathway from protonated ethylamine, and is the only fragment observed in metastable decomposition studied by Bouchoux *et al.* [13]. In their study the reaction was found to be an almost pure β elimination, nearly without hydrogen/deuterium (H/D) scrambling, unlike protonated propylamine, where hydrogen transfer to ammonia is found to take place from all positions of the alkyl chain [23]. Our labeling experiments (spectra not shown here) support the mechanism proposed by Bouchoux *et al.* [13], although some ($\sim$10%) H/D scrambling takes place. The complexity of our data

does not allow us to quantify the amount of scrambling more precisely.

The energetics of the N_2H^+/ethylamine system allow for the following series of events to take place:

$$N_2H^+ + CH_3CH_2NH_2 \rightarrow CH_3CH_2NH_3^+ + N_2 \quad (13)$$

$$CH_3CH_2NH_3^+ \rightarrow C_2H_5^+ + NH_3 \quad (14)$$
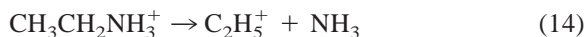
The labeling experiments (N_2D^+, data not shown) show that the ethyl cation is formed almost uniquely without H/D scrambling. This indicates a direct bond scission mechanism, without the need of passing through either of the complexes $[CH_2CH_2 \cdots H \cdots NH_3]^+$ (**14**) or $[C_2H_5^+ \cdots NH_3]$ (**18**). In their study of protonated ethanol, Mason *et al.* [22] found evidence for direct bond scission from cold ions. However, with hot ions of higher internal energies, they found that scrambling occurs, pointing to participation of an ion–molecule complex. The quite substantial amount of $C_2H_3^+$ is in accord with kinetic considerations. The tight transition state required for low energy C_2H_4 loss makes the direct
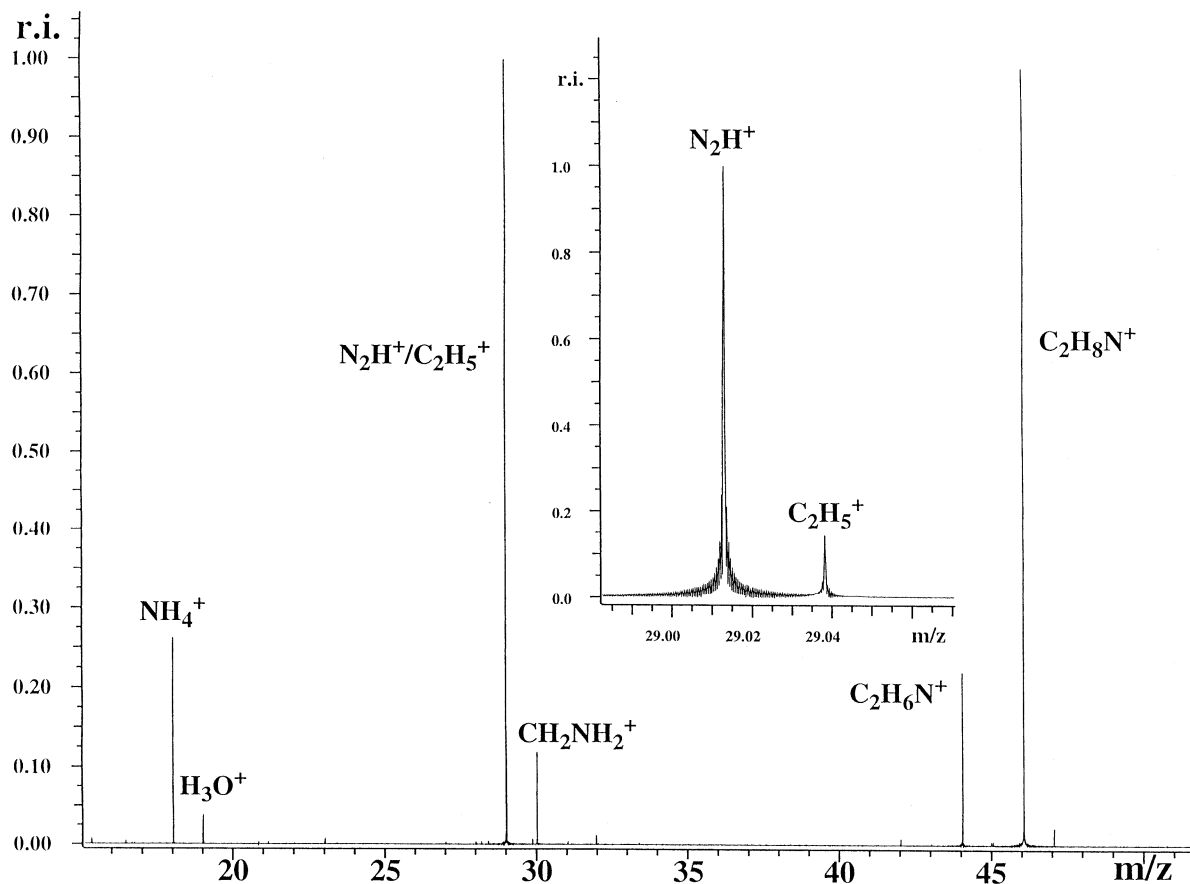
Fig. 6. Mass spectrum obtained after 20 s in the reaction between N_2H^+ and ethylamine. The insert is an enlargement of the *m/z* 29 area where both the N_2H^+ and $C_2H_5^+$ peaks are resolved.

bond scission for NH_3 loss a better candidate the higher the energy is. The lack of hydrogen interchange between the ethyl and the amine function is in agreement with an earlier study of larger protonated amines [24] and the rationalisation presented therein.

At first glance it appears puzzling that the reaction between the oxonium ion and ethylamine (Fig. 5) gives rise to $C_2H_5^+$, because judging from Fig. 4 there is not enough energy for the two step process of proton transfer followed by C–N bond scission. By taking an alternative route into consideration the puzzle is solved:

$$H_3O^+ + CH_3CH_2NH_2 \rightarrow CH_3CH_2NH_3^+ \cdots OH_2 \quad (15)$$

$$\rightarrow C_2H_5^+ + HO - H \cdots NH_3 \quad (16)$$
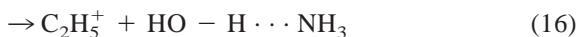
In this mechanism, the bond dissociation energy of the water/ammonia dimer compensates for the apparently unfavourable thermochemistry of proton transfer followed by C–N bond dissociation.

4.3.2. The $CH_2NH_2^+$ ion

The loss of alkanes from protonated amines is thermochemically favoured, but is generally not observed in studies of metastable protonated amines [3,13,25]. Upon collisionally induced decomposition alkane loss is observed [26]. The transition structure **TS(4/17)** leading to methane loss [reaction (11)] shows that the nitrogen bonded hydrogen moves notably toward the methyl group before the TS is reached. Such 1,2-methane eliminations are known
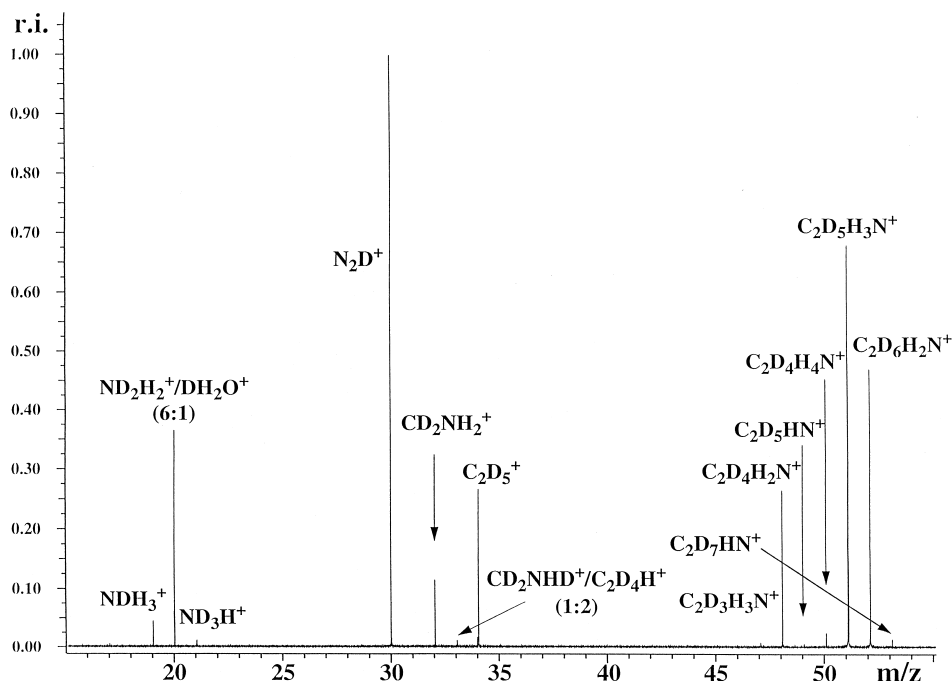
Fig. 7. Mass spectrum obtained after 20 s in the reaction between N_2D^+ and deuterated ethylamine, $CD_3CD_2NH_2$.

from the literature to have high barriers [3,27,28]. On the other hand, the bimolecular reaction [reaction (7)] where CH_3^- is abstracted in a direct encounter between the proton donor and ethylamine, proceeds with a small or zero barrier, making this the most facile reaction path. In the investigation of the chemical ionisation of several C_3 to C_5 amines it was concluded that this was the most probable source of immonium ions [3].

The immonium ion $CH_2NH_2^+$ (m/z 30.034) is visible in both Figs. 5 and 6. To clarify whether or not the bimolecular reaction is the origin of the signal, and to see if a more energetic proton transfer could make the unimolecular reaction feasible, reactions with deuterated proton donors were performed. The reaction between N_2D^+ and $CD_3CD_2NH_2$ is shown in Fig. 7. If only the unimolecular path is available and if the H and D atoms are distributed statistically (neglecting isotope effects), there is a 1:2 ratio of $CD_2NH_2^+$ (m/z 32.046) to CD_2NHD^+ (m/z 33.053). The observed ratio is 25:1, pointing in favour of direct

bimolecular abstraction of CH_3^- as the source of the immonium ion. Complementary data for $N_2D^+ + CH_3CH_2NH_2$ supports the conclusion.

4.3.3. The $C_2H_6N^+$ ion

The same argument can be used for the formation of the $C_2H_6N^+$ ion. The ratio of $C_2H_2D_4N^+$ (m/z 48.075) and $C_2HD_5N^+$ (m/z 49.084) formed in the reaction between N_2D^+ and $CD_3CD_2NH_2$ in Fig. 7 is 45:1, not 1:2, as would be expected for the two step unimolecular loss of H_2. Reactions with $CH_2CD_2NH_2$ and $CD_3CH_2NH_2$ were performed to indicate whether the $C_2H_6N^+$ ion (m/z 44.050) is formed by abstraction of a hydride from the α or β carbon.

This information was provided from the reaction between $CD_3CH_2NH_2$ and H_3O^+, as shown in Fig. 8. The insert is an enlargement of the mass range 46–48. A weak signal for removal of the α hydrogen giving $C_2D_3H_3N^+$ (m/z 47.068) and a very weak signal for removal of the β hydrogen giving $C_2D_2H_4N^+$ (m/z 46.062) are observed in the ratio 7:1. The signals are
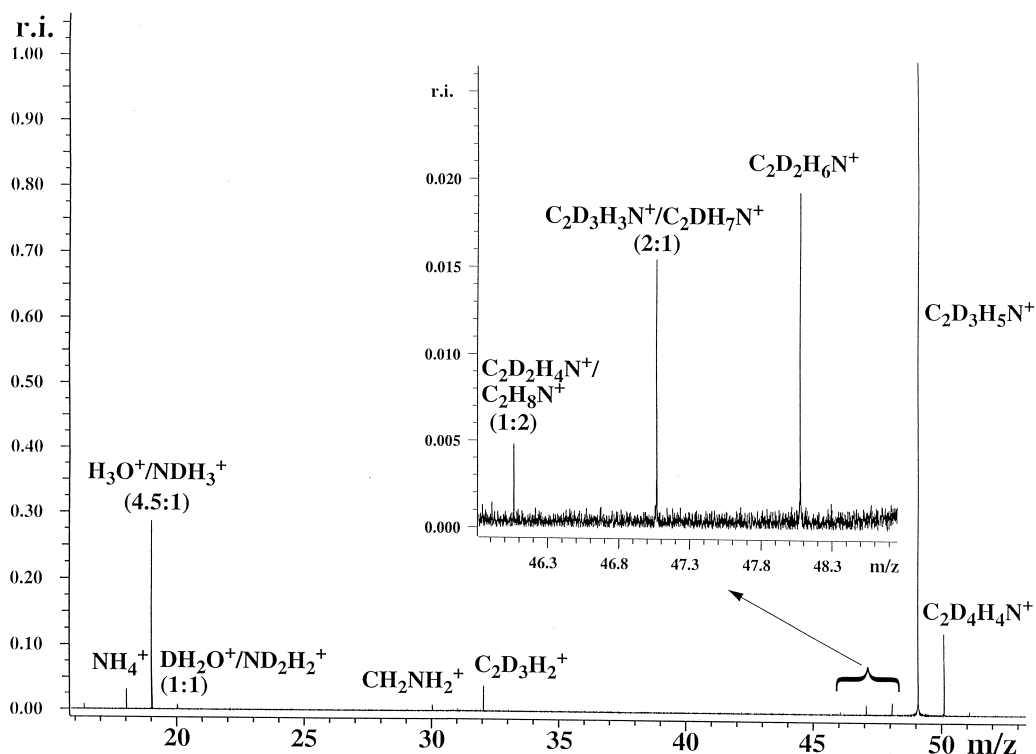
Fig. 8. Mass spectrum obtained after 20 s in the reaction between H_3O^+ and ethylamine deuterated on the β carbon, $CD_3CH_2NH_2$. The insert is an enlargement of the mass range 46 to 48; see text for details.

slightly obscured in the figure by H/D-exchange ions from the protonated molecular ion, yielding $C_2DH_7N^+$ (*m/z* 47.071) and $C_2H_8N^+$ (*m/z* 46.065).

The reaction between $CH_3CD_2NH_2$ and N_2H^+ is illustrated in Fig. 9. In this case, removal of the α hydrogen gives rise to the ion $C_2H_5DN^+$ (*m/z* 45.056), whereas removal of the β hydrogen yields $C_2H_4D_2N^+$ (*m/z* 46.062). These reactions are more prominent with N_2H^+ as the donor, and it is obvious that the removal of the α hydrogen is the more facile reaction, although both reactions take place. This is also supported by the computational findings that the transition structures for β-hydrogen abstraction are higher in energy and more strained than those for α-hydrogen abstraction. The experimental data for the reactions between $CH_3CD_2NH_2$ and H_3O^+ and $CD_3CH_2NH_2$ and N_2H^+ points in this direction.

5. Conclusion

Proton transfer and proton transfer induced reactions from ethylamine have been investigated. Two different proton donors (H_3O^+ and N_2H^+) were employed. The calculated theoretical model is supported by deuterium labeling experiments using FTICR mass spectrometry. Even though the exothermic proton transfer to the amine group of ethylamine is the dominant process, it turns out that atoms of the alkyl group are also susceptible to proton attack. This is especially facile with N_2H^+ as proton donor, for which the hydride and methide abstractions are quite exothermic and have favourable barriers. The more exothermic abstraction of the hydrogen on the α carbon dominates over the hydride abstraction from the β carbon, which is hindered by the demand for a
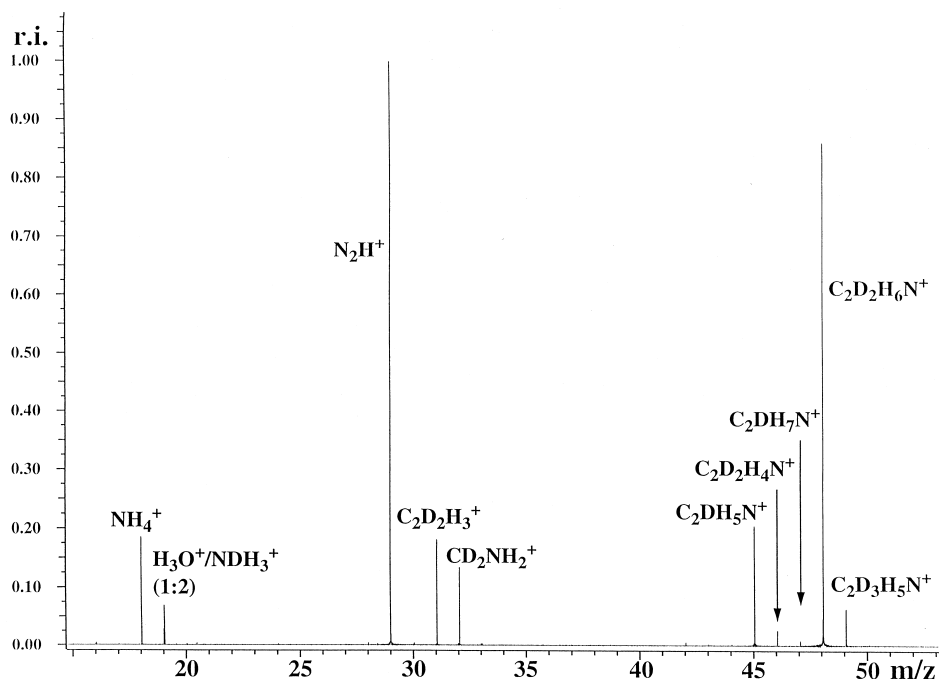
Fig. 9. Mass spectrum obtained after 20 s in the reaction between N_2H^+ and ethylamine deuterated on the α carbon, $CH_3CD_2NH_2$.

more strained transition structure. Chemical ionisation of ethylamine is thus demonstrated to be quite complex.

The ions NH_4^+ and $C_2H_5^+$ appear to come mainly from unimolecular fragmentation subsequent to protonation on nitrogen. Deuterium labeling experiments support a β-elimination mechanism for NH_4^+ formation by loss of ethene, and a direct bond scission for $C_2H_5^+$ formation by loss of ammonia. The $CH_2NH_2^+$ and $C_2H_6N^+$ ions are found to originate from methide and hydride abstraction, respectively, and are not fragmentation products of protonated ethylamine.

Of the $CH_3CH_2NH_3^+$ ions, relatively few decompose unimolecularly. Because fragmentation is steered by the amount of energy deposited into protonated ethylamine upon formation, simple analysis of the $[MH^+]$:[fragment ion] ratio indicates that in the case of N_2H^+, on the order of 50% of the energy ends up as internal energy. In the case of H_3O^+ a larger fraction of the available energy ends up in MH^+.

Acknowledgements

References

[1] M.S.B. Munson, F.H. Field, J. Am. Chem. Soc. 88 (1966) 2621.
[2] A.G. Harrison, Chemical Ionization Mass Spectrometry, 2nd edn., CRC, Boca Raton, FL, 1992.
[3] E.J. Reiner, R.A. Poirier, M.R. Peterson, I.G. Csizmadia, A.G. Harrison, Can. J. Chem. 64 (1986) 1652.
[4] H.E. Audier, G. Bouchoux, P. Mourgues, F. Penaudberruyer, Org. Mass Spectrom. 27 (1992) 439.
[5] J.L. Fry, G.J. Karabatsos, in Carbonium Ions, G.A. Olah, R.P. von Schleyer (Eds.), Interscience, New York, 1968, Vol. 2.
[6] C.D. Nenitzescu, in Carbonium Ions, G.A. Olah, R.P. von Schleyer (Eds.), Interscience, New York, 1968, Vol. 2.

[7] T.F. Magnera, P. Kebarle, in Ionic Processes in the Gas Phase, M.A. Almoster-Ferreira (Ed.), Reidel, Dordrecht, 1984, pp. 135.

[8] M. Meot-Ner, in Gas Phase Ion Chemistry, M.T. Bowers, (Ed.), Academic, New York, 1979, Vol. 1, pp. 197.

[9] C.I.F. Watt, Adv. Phys. Org. Chem. 24 (1988) 57.

[10] C. Berg, W. Wachter, T. Schindler, C. Kronseder, G. Niedner-Schatteburg, V.E. Bondybey, Z. Herman, Chem. Phys. Lett. 216 (1993) 465.

[11] M.V. Frash, V.N. Solkan, V.B. Kazansky, J. Chem. Soc. Faraday Trans. 93 (1997) 515.

[12] C. Matthias, K. Weniger, D. Kuck, Int. J. Mass Spectrom. (2000) . . .(this issue).

[13] G. Bouchoux, F. Djazi, M.T. Nguyen, J. Tortajada, J. Phys. Chem. 100 (1996) 3552.

[14] L.J. deKoning, N.M.M. Nibbering, S.L. vanOrden, F.H. Laukien, Int. J. Mass Spectrom. Ion Processes 165 (1997) 209.

[15] T. Su, W. Chesnavich, J. Chem. Phys. 76 (1982) 5183.

[16] M.J. Frisch, G.W. Trucks, H.B. Schlegel, P.M.W. Gill, B.G. Johnson, M.A. Robb, J.R. Cheeseman, T. Keith, G.A. Petersson, J.A. Montgomery, K. Raghavachari, M.A. Al-Laham, V.G. Zakrzewski, J.V. Ortiz, J.B. Foresman, J. Cioslowski, B.B. Stefanov, A. Nanayakkara, M. Challacombe, C.Y. Peng, P.Y. Ayala, W. Chen, M.W. Wong, J.L. Andres, E.S. Replogle, R. Gomperts, R.L. Martin, D.J. Fox, J.S. Binkley, D.J. Defrees, J. Baker, J.P. Stewart, M. Head-Gordon, C. Gonza-lez, J.A. Pople, GAUSSIAN 94, Revision E.2, Gaussian Inc., Pittsburgh, PA, 1995.

[17] C. Möller, M.S. Plesset, Phys. Rev. 46 (1934) 618.

[18] L.A. Curtiss, K. Raghavachari, G.W. Trucks, J.A. Pople, J. Chem. Phys. 94 (1991) 7221.

[19] J.A. Pople, A.P. Scott, M.W. Wong, L. Radom, Isr. J. Chem. 33 (1993) 345.

[20] W.G. Mallard, P.J. Linstrom, (Eds.), NIST Chemistry Web-Book, NIST Standard Reference Database Number 69, National Institute of Standards and Technology, Gaithersburg, MD, 1998 (http://webbook.nist.gov).

[21] D.J. Swanton, D.C.J. Marsden, L. Radom, Org. Mass Spectrom. 26 (1991) 227.

[22] R.S. Mason, J.C. Naylor, J. Phys. Chem. A 102 (1998) 10 090.

[23] H.E. Audier, T.H. Morton, Org. Mass Spectrom. 28 (1993) 1218.

[24] A.G. Harrison, Org. Mass Spectrom. 22 (1987) 637.

[25] R.D. Bowen, A.G. Harrison, E.J. Reiner, J. Chem. Soc. Perkin Trans. 2 (1988) 1009.

[26] E.J. Reiner, A.G. Harrison, R.D. Bowen, Can. J. Chem. 67 (1989) 2081.

[27] M.T. Nguyen, L.G. Vanquickenborne, G. Bouchoux, Int. J. Mass Spectrom. Ion Processes 124 (1993) R11.

[28] M.T. Nguyen, G. Bouchoux, J. Phys. Chem. 100 (1996) 2089.